Water Resour Manage (2012) 26:2851–2866
DOI 10.1007/s11269-012-0052-y

The Importance of Data Acquisition Techniques in Saltwater Intrusion Monitoring

M. Mastrocicco · B. M. S. Giambastiani · P. Severi · N. Colombani

Received: 26 July 2011 / Accepted: 8 May 2012 /
Published online: 24 May 2012

Abstract A detailed vertical characterization of a coastal aquifer was performed along a flow path to monitor the seawater intrusion. Physico-chemical logs were obtained by both open-borehole logging (OBL) and multilevel sampling technique (MLS) via straddle packers in piezometers penetrating the coastal aquifer of the Po River Delta, Italy. The open borehole logs led to a satisfactory reconstruction of the extent of the fresh-saltwater interface but provided a misleading characterization of the distribution of redox environments within the aquifer. On the contrary, good fits between sedimentological, stratigraphycal and physico-chemical data were obtained using the straddle packers devices. This study demonstrates that, within coastal shallow aquifers evenly recharged by irrigation canals, the simple and economical OBL technique can lead to misleading results when used to characterize density dependent groundwater stratification but is deemed adequate for preliminary assessments of the saltwater wedge location.

Keywords Coastal aquifer · Groundwater quality · Seawater intrusion · Hydrochemistry · Multilevel sampling

1 Introduction

The saltwater intrusion into coastal aquifers may arise from both natural and anthropogenic sources (Lenahan and Bristow 2010) and is a widespread phenomenon that gradually causes

M. Mastrocicco · B. M. S. Giambastiani · N. Colombani
Earth Sciences Department, University of Ferrara, Via Saragat 1, 44122 Ferrara, Italy

P. Severi
Geological, Seismic and Soil Survey, Emilia Romagna Region, Viale della Fiera 8, 40127 Bologna, Italy

N. Colombani (✉)
CIRSA – Interdepartmental Centre for Environmental Sciences Research, University of Bologna,
Via San Alberto 163, 48100 Ravenna, Italy
e-mail: clo@unife.it

the problem of groundwater and aquifer salinization. The increasing demand of freshwater in coastal areas has intensified the research on saltwater intrusion (Barlow and Reichard 2010; Custodio 2010; Post and Abarca 2010). In coastal areas groundwater has gained increasing attention as a source of water supply, owing to its relatively low vulnerability to pollution in comparison to surface water as well as its relatively large storage capacity (Dillon 2005). However, in the absence of sustainable water resource management schemes, uncontrolled land-use activities and over-exploitations can lead to significant and long-lasting deteriorations in coastal water resources and ecosystems (Candela et al. 2009; Grassi et al. 2007; Park et al. 2005).

A key issue to understanding salinization processes and to properly manage groundwater resources is to correctly characterize the vertical variability of groundwater quality (Nativ and Weisbrod 1994; Netzer et al. 2011). For this reason, since 2009 the Geological Survey of the Emilia Romagna Region has developed a specific monitoring network of 30 piezometers as a means of characterizing the saltwater intrusion along the Northern Adriatic coastal aquifer (Bonzi et al. 2010).

In addition, to understand the hydrogeochemical processes occurring within a groundwater system it is necessary to: (i) define the contribution of water-sediment interactions; and (ii) quantify the anthropogenic influence on groundwater quality (Gaofeng et al. 2010). An inexpensive and fast method of obtaining depth dependent groundwater quality data is through open borehole logging (OBL). This method is employed to identify fresh-saltwater interfaces in coastal aquifers (Kim et al. 2008) and to characterize the redox zones within contaminant plumes (Jorstad et al. 2004; Schurch and Buckley 2002). Despite its apparent simplicity, the OBL technique has some limitations, most notably in coastal zones where measured values (salinity or any other water property) may well be representative of the stratified water column accumulated within the piezometer but not necessarily of the surrounding porous media (Balugani and Antonellini 2010; Kurtzman et al. 2011; Shalev et al. 2009). On the contrary, multilevel sampling (MLS) techniques are routinely applied in contaminated sites to map contaminant spreading and to quantify biogeochemical reaction pathways (Colombani et al. 2009; Henderson et al. 2009; Prommer et al. 2006; Thierrin et al. 1995), but less frequently in monitoring the saltwater intrusion in coastal areas because of their high cost and time involved.

The aim of this study is to compare the OBL technique with a more robust but more time consuming MLS technique, such as inflatable straddle packers. This work is accomplished in order to assess if the OBL is sufficient enough in gaining representative hydrogeochemical data in shallow coastal aquifers stressed by seawater intrusion and intense anthropogenic pressure.

2 Depositional Environment and Hydrodynamic Setting

The study area is situated within the Province of Ferrara and is bounded to the north by one of the Po River branches, the Po di Goro, and to the south by the brackish water marshes of the Comacchio Lagoons (Fig. 1). The surface water system consists of a dense network of west-east oriented channels and drainage ditches with pumping stations that mechanically discharge water towards the sea (Antonellini et al. 2008). Most of the territory is reclaimed land with a flat topography below sea level and is affected by natural (Carbognin and Tosi 1995; Carminati et al. 2005) and anthropogenic subsidence (Teatini et al. 2006).

The stratigraphic architecture of sediments shows consistent patterns of coastal evolution with changing sea level position. Lowering of the sea level between 125,000 and

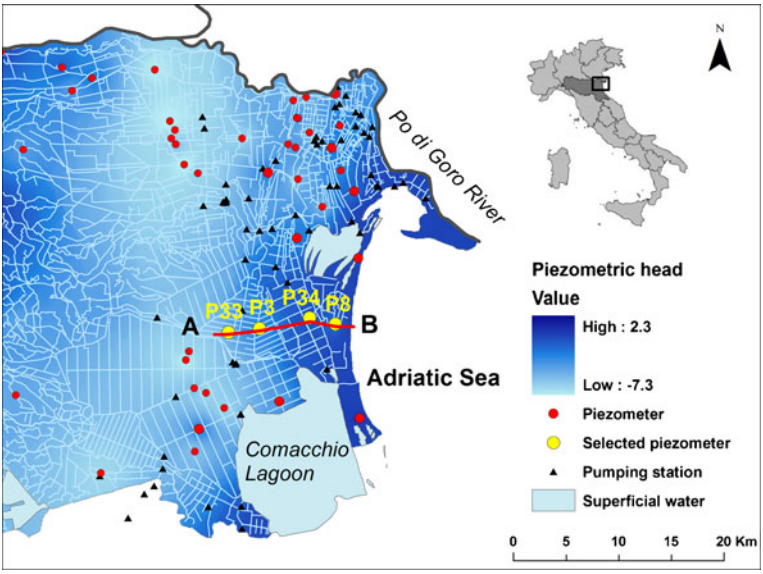

Fig. 1 Location of the study area with the piezometric contour map, canals network and borehole locations; in yellow the selected piezometers along a flow line (AB)

70,000 years ago resulted in extensive and repeated basinward shifts of facies, which can be observed across closely spaced unconformity surfaces associated with alluvial plain sedimentation (Amorosi et al. 2003). The general phase of sea level fall was interrupted by short transgressive phases, which led to the deposition of organic rich deposits (lagoons and swamps). The Holocene interglacial deposits were characterized by a retrogradational stacking pattern of coastal plain and littoral facies, which reflected landward migration of a barrier–lagoon–estuary system. The subsequent highstand deposition was characterized by extensive progradation of wave influenced deltas and strand plains (Amorosi et al. 2004).

During the last glacial lowstand, the modern coastal region was the site of middle alluvial plain sedimentation. In the contemporary coastal zone, transgressive accumulation started between 10,000 and 9,000 years ago. Back-stepping fluvial and brackish marsh deposits were followed by delta-estuarine sand bodies, influenced by the last important eustatic rise pulses. Early highstand saw the growth of large sand spits and barrier islands, progressively turning the previous bays into confined lagoons (Stefani and Vincenzi 2005).

This complex stratigraphic evolution led to a complex geometry of the aquifer. From east to west, the majority of the sedimentary units consist of a wedge of permeable sand sediments deposited in shallow marine water, littoral sands formed in the foreshore and in the adjacent beach, and sand dune systems (Antonellini et al. 2008). In the westernmost area fine continental alluvial deposits (mostly silt and clay) overlay the littoral sands (Amorosi et al. 2002; Bondesan et al. 1995).

The coastal aquifer is located mainly within the littoral sands and in the shallow marine wedge deposits. The thickness of the aquifer varies from 16 m to 22 m moving from the eastern to the western part of the study area (Fig. 2).

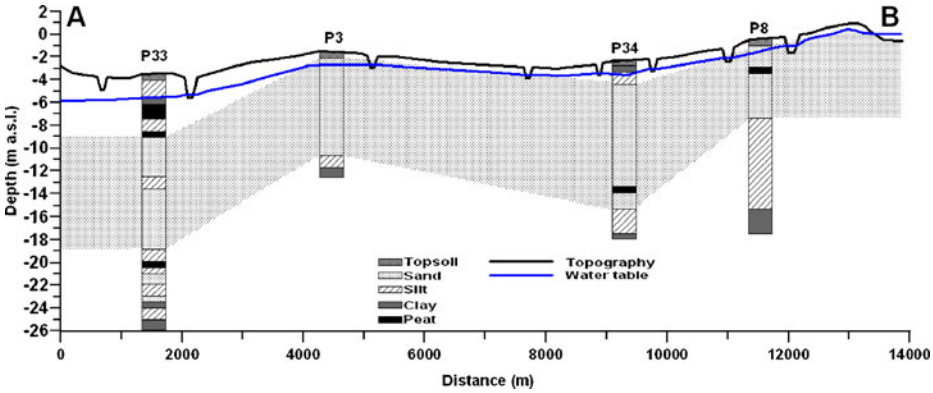

Fig. 2 Transect AB (refer to Fig. 1 for the location). Topography (DEM data), water table (monitoring data of November 2010), sandy aquifer thickness (dotted region) and stratigraphy (core logs data) are shown

3 Materials and Methods

3.1 Piezometer Installation

The four selected boreholes along transect AB (Fig. 2) are part of the regional monitoring network of the costal aquifer, which, since 2009, have been equipped with piezometers installed by the Geological Survey of the Emilia-Romagna Region (Italy).

All wells (5 cm inner diameter) were screened from 1 m below ground level (b.g.l.) to a maximum of 22 m b.g.l. to fully penetrate the aquifer. The screens were not surrounded by a siliceous gravel pack to prevent cross contamination between sampling points, while a geotextile sock was used to minimize the piezometer clogging. The piezometers were sealed with a mixture of cement and bentonite at the top to prevent surface-water infiltration. In two boreholes, P33 and P34, core samples were collected every meter or when a change in sediments was recognized. Samples were stored in a cool box at 4 °C and immediately transported to the laboratory for sediment analysis.

3.2 Stratigraphycal and Sedimentological Analysis

Particle size curves were obtained using a sedimentation balance for the coarse fraction and an X-ray diffraction sedigraph 5100 Micromeritics for the finer fraction; the two regions of the particle size curve were connected using the computer code SEDIMCOL (Brambati et al. 1973). To describe grain size distribution analysis, the median of the average grain radius (expressed in φ), the 10th and 60th percentile of the cumulative curve (d_{10} and d_{60} expressed in φ) and the sorting were calculated. The organic matter content of the sediments was measured by dry combustion (Tiessen and Moir 1993).

The hydraulic conductivity (k) of piezometers P33 and P34 was measured in the field every 1 m by using an 800 L straddle packers system (Solinst, Canada) with sampling window of 0.2 m connected to a submersible centrifuge pump able to deliver 20 l/min. The head loss was measured by a levelogger LTC (Solinst, Canada) placed in between the two packers. The levelogger accuracy is ±0.01 m with a maximum pressure range of 10 m; below this depth the measurements are not reliable. Thus k values could not be accurately measured towards the bottom of the aquifer

and were limited to 10 m of saturated zone. k values (m/s) were derived from the equation (Bureau of Reclamation 2001):

$$k = \frac{Q}{C_s r \Delta h} \tag{1}$$

where C_s (-) is the conductivity coefficient for semi-spherical flow in saturated materials through partially penetrating cylindrical test wells and for these condition is equal to 28, r (m) is the radius of the test well, Δh (-) is the head hydraulic gradient between static head and steady state head under pumping condition.

The water content was measured in saturated conditions gravimetrically after heating for 24 h at 105 °C (Danielson and Sutherland 1986). Laboratory porosity measurements (n) on core samples are often affected by errors, as many sampling methods alter the structure, packing and compaction of the sediment sample (Vienken and Dietrich 2011). Hence porosity values were also computed using the following empirical equation (Vukovic and Soro 1992):

$$n_v = 0.225(1 + 0.83\eta) \tag{2}$$

where η stand for uniformity coefficient, defined as $d_{60}[\varphi]/d_{10}[\varphi]$.

The effective porosity (n_e) was estimated with the formula (Worthington 1998):

$$n_e = n - CBW \tag{3}$$

where CBW is the clay-bounded water, which comprises electrochemically bound water from clay surfaces and interlayers. The CWB varies in volume according to the clay-type, and the salinity of the formation water and can be estimated from (Hill et al. 1979):

$$CBW = n \times \left(0.6425 \times \sqrt{S} + 0.22\right) \times CEC \tag{4}$$

where S is the salinity (g/l) and CEC is the Cation Exchange Capacity (meq/ml of pore space).

Finally, the pore water velocity along each piezometer was calculated following Darcy's law in the form of freshwater heads:

$$v = \frac{k_f \times \overrightarrow{i}}{n_e} \tag{5}$$

where v is the average pore water velocity (m/y), $\overrightarrow{i}$ is the freshwater hydraulic head gradient (-), n_e is the effective porosity (-) and k_f is the fresh water hydraulic conductivity (m/y). By assuming that salinity variations have a negligible effect on the groundwater kinematic viscosity, viscosity k_f values can be considered similar to field-measured values of hydraulic conductivity (Post et al. 2007). In order to compute velocity values (v and v_v in Tables 3 and 4), k values were obtained by Eq. 1 while effective porosity values (n_e and n_{ev}) were calculated for each core sample by Eq. 3 using both the measured total porosity (n) and the calculated total porosity by Vukovic and Soro (1992) (n_v). For the shallow coastal aquifer, a regional $\overrightarrow{i}$ influenced by the dewatering stations equal to 0.4‰ was applied.

3.3 Open Borehole Profiles and Multi-Level Sampling

In order to obtain the OBL profiles, a Hydrolab MS-5 (OTT, Germany) water quality probe was lowered into four boreholes to simultaneously record temperature, electrical conductivity (EC), dissolved oxygen (O_2), redox potential (Eh), pH and salinity. The Hydrolab MS-5

water quality probe consists of six sensors and a data transmitter mounted inside a 4.4 cm diameter housing, with a 30 m long underwater cable and an YSI interface (YSI, California) at the ground surface. The Eh was corrected to the standard H^+ electrode potential. Logging was carried out by lowering manually the multi-parameter probe into four piezometers P3, P8, P33, and P34 (Fig. 1). After a 5 min wait, the six parameters were simultaneously acquired every 1 m depth. The hydrochemical log measurements were made under natural conditions, without purging the piezometers before the tests.

To acquire the MLS profiles, groundwater samples were collected every 1 m from the four piezometers, by using an 800 L straddle packers system (Solinst, Canada). The samples were collected via a low-flow technique using an inertial pump, after measuring the groundwater static level and purging of about 5 L. For each sample hydrochemical parameters were acquired in situ by using a Hydrolab flow cell connected to the Hydrolab MS-5 probe. Groundwater samples were then collected, filtered through 0.22 μm Dionex polypropylene filters, stored in a cool box at 4 °C and immediately transported to the laboratory for chloride analysis. Chloride was analyzed using an isocratic dual pump ion chromatography ICS-1000 Dionex, equipped with an AS9-HC 4×250 mm high capacity column and an ASRS-ULTRA 4 mm self-suppressor for anions. An AS-40 Dionex auto-sampler was employed for the analyses, Quality Control (QC) samples were run every 10 samples and the standard deviation for all QC samples run was greater than 4 %.

To compare data obtained by OBL and MLS techniques, the absolute residuals (the absolute value observed using MLS minus the absolute value observed using OBL at the same depth) and the linear regression coefficient (R^2) with respect to the line $Y_{OBL} = X_{MSL}$ was calculated for each parameter analyzed.

3.4 Continuous Monitoring of Piezometric Heads and Sea Level

In order to define groundwater temporal variations due to tidal fluctuations, a STS datalogger DL/N Series 70 was placed in piezometer P8, located close to the coastline (≈1,400 m inland). The datalogger was set up for continuous barometric compensated level measurement and electrical conductivity (one record per hour). The probe was placed in the saturated zone at 4.5 m b.g.l. to capture groundwater fluctuations. The online data from Ravenna mareographer of ISPRA were used (www.retemareografica.it) to compare groundwater fluctuations with tidal variations. Sea level data from Ravenna mareographer have an average lag phase of about 15 min with respect to the mareographer of Porto Garibaldi (http://www.provincia.fe.it/sito?nav=293&doc=E93B184E4E0ACBFCC125766900371819), positioned in proximity of the piezometer P8.

4 Results and Discussion

4.1 Hydrostratigraphycal Characterization

Tables 1 and 2 report the grain size distribution analysis performed on the samples of piezometers P33 and P34, respectively. The core sample analysis reveals a certain heterogeneity of the core logs, with very poorly sorted silty clay and peat lenses overlaying a highly permeable well sorted sandy layer typical of high energy depositional environments, such as coastal environment (dunes and beaches), intercalated with poorly sorted sandy silt lenses. The sandy and sandy silt layers constituting the aquifer, are underlined throughout by an aquitard, in agreement with previous studies (Amorosi et al. 2003). Porosity values (Tables 1 and 2) range

between 18 % and 76 %, with high values due to the presence of peat layers exhibiting a high organic matter content (OM%).

Tables 3 and 4 summarize the parameters measured (k) and derived from empirical formulas (n_e) used to calculate the mean groundwater flow velocities in piezometers P33 and P34 respectively. The estimated Peclet number (P_e), defined as (Bear 1972):

$$\mathrm{P_e} = \mathrm{v\,d/D_f} \tag{6}$$

where d is the average diameter of the grains constituting the aquifer (m), D_f is the diffusion coefficient in pure water (m^2/s) and v is the pore water flow velocity (m/s), is always below 1 and therefore the flow is dominated by diffusion-driven processes, or at least the role of diffusion is comparable to that of mechanical dispersion (Appelo and Postma 2005).

The estimated flow velocities show that seawater intrusion is proceeding inland at a very slow rate due to the effects of the dewatering stations draining the recently reclaimed area of the Ferrara Province (Fig. 1). This confirms that the salinity present in the coastal shallow aquifer is mostly due to interactions between water and sediments deposited during the last transgressive period that was characterized by landward migration of a barrier–lagoon–estuary system.

Table 1 Core sample analyses of P33 borehole

i.d.	Elevation m a.s.l	O. M. %	Sand %	Silt %	Clay %	*Median* φ	d_{10} φ	d_{60} φ	Sorting φ
C01	−4.93	2.12	22.28	56.36	21.36	5.90	9.25	5.00	2.28
C02	−5.70	3.06	2.48	67.47	30.05	6.74	10.13	5.63	2.02
C03	−6.08	6.15	0.39	46.70	52.91	8.55	11.88	7.63	2.26
C04	−6.35	17.17	0.31	16.68	83.01	9.49	10.75	9.50	1.56
C05	−6.70	62.50	6.90	63.10	30.00	7.80	10.10	7.8	2.00
C06	−7.53	6.59	1.26	70.59	28.15	7.13	11.00	6.00	2.31
C07	−8.60	6.06	1.46	57.77	40.77	7.95	11.75	6.88	2.48
C08	−9.40	5.80	80.48	10.74	8.78	3.36	7.50	2.50	1.96
C09	−10.53	1.59	70.67	23.80	5.53	3.59	7.00	2.50	1.88
C10	−12.45	0.80	96.52	2.43	1.05	2.25	3.00	2.00	0.47
C11	−13.65	3.21	26.98	59.16	13.86	5.39	8.75	5.00	2.29
C12	−14.23	1.60	92.72	6.30	0.98	3.12	3.88	3.00	0.56
C13	−14.80	2.18	62.65	24.10	13.25	4.50	8.88	3.25	2.22
C14	−16.50	2.30	62.78	28.64	8.58	4.39	7.75	3.50	1.79
C15	−18.80	3.16	63.18	30.62	6.20	4.05	6.50	3.63	1.37
C16	−19.40	3.22	76.39	18.09	5.52	3.62	6.25	3.25	1.38
C17	−20.10	4.07	29.73	44.45	25.82	6.07	9.75	5.50	2.59
C18	−20.90	37.27	4.25	51.18	44.57	7.91	10.63	7.25	2.10
C19	−21.60	6.48	50.36	34.67	14.97	5.02	9.25	3.75	2.23
C20	−23.15	6.22	12.26	59.50	28.24	6.82	10.63	6.00	2.45
C21	−23.90	4.94	55.83	38.92	5.25	4.26	6.38	3.75	1.27
C22	−25.20	5.71	5.59	65.83	28.58	6.95	7.13	5.75	2.42
C23	−25.90	5.45	0.45	29.68	69.87	9.28	12.13	8.50	2.09

Table 2 Core sample analyses of P34 borehole

i.d.	Elevation m a.s.l	O. M. %	Sand %	Silt %	Clay %	*Median* φ	d_{10} φ	d_{60} φ	Sorting φ
C01	−3.80	7.81	1.44	42.85	55.71	8.56	11.75	7.75	2.33
C02	−4.60	7.68	7.38	50.52	42.10	7.66	11.13	6.63	2.62
C03	−6.50	1.65	92.69	5.85	1.46	2.80	3.63	2.75	0.58
C04	−7.50	1.09	96.64	2.73	0.63	2.18	2.88	2.00	0.46
C05	−8.50	1.34	94.56	4.00	1.44	2.09	3.00	2	0.69
C06	−12.50	5.04	64.68	29.63	5.69	4.03	6.63	3.50	1.40
C07	−14.10	10.61	55.58	34.08	10.34	4.61	8.13	3.63	1.99
C08	−15.50	4.87	71.51	23.55	4.94	3.99	6.38	3.50	1.26
C09	−16.50	6.67	13.76	48.86	37.38	6.75	10.25	5.25	2.47

4.2 Tidal Forcing Effects on Groundwater Fluctuation

Figure 3 shows the relationship between tidal fluctuation and groundwater level in the piezometer P8 from August 2009 to May 2010. From this plot it is clear that the tidal amplitude is approximately 0.4 m, the tidal range is 0.8 m and the average tidal level is 0.18 m a.s.l., with the highest sea levels occurring during winter time due to storm events (Martinelli et al. 2010; National Marine Hydrographic Institute 1994). The piezometric heads recorded in the piezometer P8 meanwhile are quite stable in summer and early autumn, with a sudden 0.5 m decline in November 2009 and a steep rise in April 2010, following the irrigation/drainage canals regime. The general canals regime is regulated to provide freshwater for agricultural purposes during the growing season and to drain precipitation events during the wet season. Overall the maximum piezometric head variation during the monitoring period was 0.89 m with a mean value of −1.66 m a.s.l.. The response to precipitation events is good, with a groundwater level peak after every rainfall. During the winter time the groundwater level rapidly decrease in absence of precipitations since the aquifer is not recharged by surface canals. In addition, in this season both sea level and

Table 3 Values of measured total porosity (*n*), calculated total porosity by Vukovic and Soro (1992) (n_v), respective effective porosity (n_e, n_{ev}) and pore water velocity (*v* and v_v), and measured hydraulic conductivity (k) in P33 borehole

i.d.	Elevation m a.s.l	*n* –	n_v –	n_e –	n_{ev} –	*k* m/s	*v* m/y	v_v m/y
C05	−6.70	0.76	0.37	0.11	0.05	$1.1e^{-4}$	12.8	26.5
C08	−9.40	0.33	0.29	0.27	0.24	$2.1e^{-4}$	9.5	10.9
C09	−10.53	0.18	0.29	0.16	0.26	$4.8e^{-5}$	3.8	2.3
C10	−12.45	0.27	0.35	0.26	0.34	$1.2e^{-4}$	5.6	4.3
C11	−13.65	0.24	0.33	0.19	0.27	$2.8e^{-5}$	1.9	1.3
C12	−14.23	0.25	0.37	0.24	0.35	$2.6e^{-5}$	1.4	0.9
C13	−14.80	0.19	0.29	0.15	0.24	$7.5e^{-6}$	0.6	0.4
C14	−16.50	0.20	0.31	0.17	0.26	$4.3e^{-6}$	0.3	0.2
C15	−18.80	0.21	0.33	0.18	0.28	$2.3e^{-6}$	0.2	0.1

Table 4 Values of measured total porosity (*n*), calculated total porosity by Vukovic and Soro (1992) (n_v), respective effective porosity (n_e, n_{ev}) and pore water velocity (v and v_v), and measured hydraulic conductivity (k) in P34 borehole

i.d.	Elevation m a.s.l	n –	n_v –	n_e –	n_{ev} –	k m/s	v m/y	v_v m/y
C03	−6.50	0.26	0.37	0.24	0.34	$6.7e^{-5}$	3.6	2.5
C04	−7.50	0.25	0.35	0.24	0.34	$6.2e^{-5}$	3.3	2.3
C05	−8.50	0.24	0.35	0.23	0.33	$1.3e^{-5}$	0.7	0.5
C06	−12.50	0.25	0.32	0.21	0.27	$1.9e^{-6}$	0.1	0.1
C08	−15.50	0.23	0.33	0.19	0.27	$3.0e^{-6}$	0.2	0.1

groundwater table fluctuate accordingly with the "inverted barometric effect" (Balugani and Antonellini 2011). The low piezometric head variation during the hydrologic year shows that the unconfined aquifer is affected by the channel network and the fact that values are always below the mean sea level confirm that the groundwater flow direction is always inland, favoring seawater intrusion. The right panel in Fig. 3 indicates the results of the analysis during a shorter period of only 1 week, when the hydrometric level of the nearby canal was stable and precipitation absent. In this period of time there is no evident correlation with the tidal fluctuation, in agreement with a recent study (Balugani and Antonellini 2011) which demonstrates that the tidal fluctuations are completely dampened within 200 m from the coast line. During this period the recorded groundwater oscillations were most probably due to variations of the canal's hydrometric level. It can therefore be inferred that since P8 is the

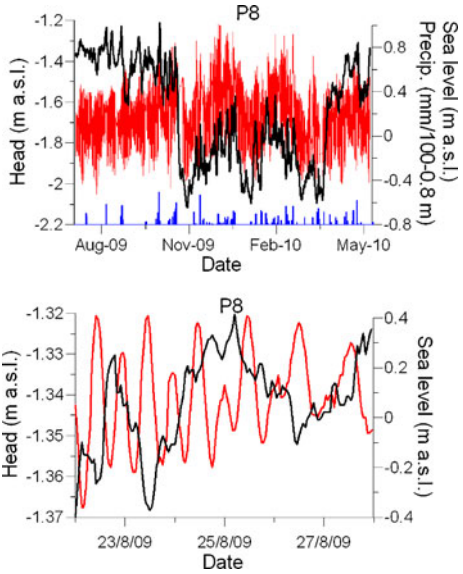

Fig. 3 Plots of continuous piezometric head monitoring of piezometer P8 (*black line*) and sea level (*red line*). The left plot shows the entire monitoring period with also the precipitation events, while the right plot shows a zoomed timeframe of 1 week when the tidal oscillation is more evident. Note that the y scales have different ranges and precipitations are scaled, offset and plotted in the sea level y axis

nearest piezometer to the coastline, the other piezometers along the monitored transect are not affected by tidal fluctuations.

4.3 Hydrogeochemical Monitoring

Figure 4 shows the salinity profiles for the four piezometers along transect AB (Figs. 1 and 2). Considering both OBL and MLS profiles, the aquifer overall displays fresh water (salinity <0.5 g/l) in the uppermost section of P3 and P8, from the top of the water table down to −9 and −6 m a.s.l. respectively, and a transition zone of brackish water (from 0.5 to 30 g/l) with a thickness ranging from 1 to 4 m. As expected, the transition zone is thin due to the minimal tidal fluctuations in this particular area of the Adriatic Sea, as explained above. Finally, saline (from 30 to 50 g/l) to hypersaline (>50 g/l) water is present in the remaining thickness of the aquifer (Barlow 2003).

Overall the absolute salinity residual for all the piezometers is 4.31 g/l and the R^2 is 0.92, which is deemed an acceptable goodness of fit between the two techniques.

Since the two different acquisition techniques, *i.e.* the OBL and MLS methods, give approximately the same classification and distribution of the water types present in the aquifer, it follows that the OBL method can be successfully used for a preliminary determination of the position of the saltwater wedge in aquifers with normal density stratification (freshwater near the water table and saline groundwater towards the bottom).

Nevertheless, analysing in more detail the OBL salinity profiles against the MLS profiles, some considerable differences are apparent. In P8 and P34 the OBL technique displays a somewhat constant concentration profile in the lower part of the aquifer where hypersaline water is present. The MLS technique on the other hand, is able to distinguish in both

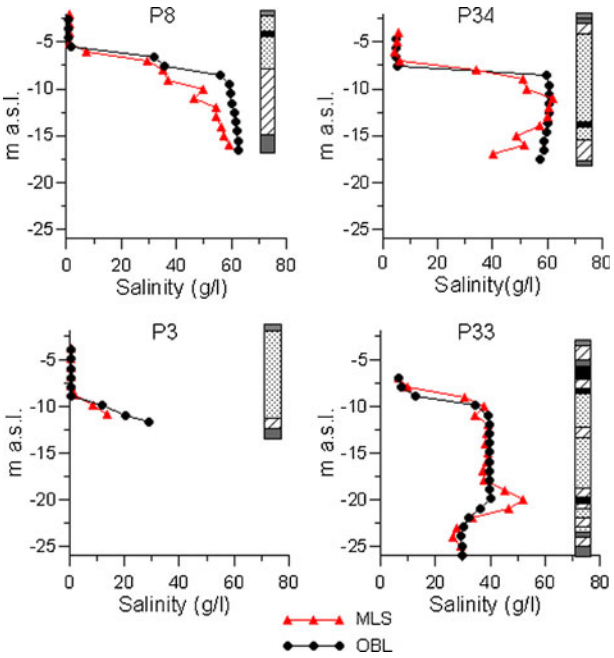

Fig. 4 Plots of salinity with MLS versus OBL data for each piezometer along transect AB; stratigraphy (core logs data) from Fig. 2 is displayed on each plot to assist the interpretation

piezometers a considerable variability in the concentration profiles. In particular, the salinity distribution in P8 slowly increases from saline (−8 m a.s.l.) to hypersaline water (−17 m a.s.l.), showing salinities always lower than the ones recorded at the same depths by OBL. In the hypersaline bottom part of the aquifer the deviation of the MLS profile from the OBL profile is even more evident; in P34 the MLS profile shows a correlation between the salinity distribution and the stratigraphy, witnessing water-sediment interactions.

Accordingly in P33, the MLS profile demonstrates that the change in sediments reflects a change in salinity: at −20 m a.s.l. salinity increases up to 53 g/l in correspondence with a peaty layer.

It is also interesting to note that by plotting the Cl^- versus salinity concentrations for all the analyzed groundwater samples (Fig. 5), a very close fit for salinity samples below seawater composition is obtained, with a R^2 value of 0.981. Using all the concentration data meanwhile results in the fit degrading to a R^2 value of 0.947. This means that along this transect, salinity can be considered representative of a conservative species (like Cl^-) only below seawater concentration, since above this concentration a large number of the observed values fall outside the 95 % confidence interval of the linear regression line (Fig. 5).

The misleading distribution of salinity values above seawater concentration recorded via the OBL technique is thought to be due to both the mixing of water into the piezometers induced by the density dependent flow and to the downward and upward movement of the probe within the borehole casing during the monitoring procedure. These bias are obviously avoided using the MLS techniques.

As for the salinity values above seawater concentration, the OBL and MLS techniques present a discordant picture of the physico-chemical parameter profiles of the coastal shallow aquifer. Figure 6 describes pH profiles collected via OBL and MLS techniques. The profiles are not in good agreement, with an absolute residual for all piezometers of 0.37 and an R^2 value of 0.72. The pH measured by MLS is regularly higher than the one measured by the OBL technique, even if in both cases the ambient groundwater is characteristic of the basic environment.

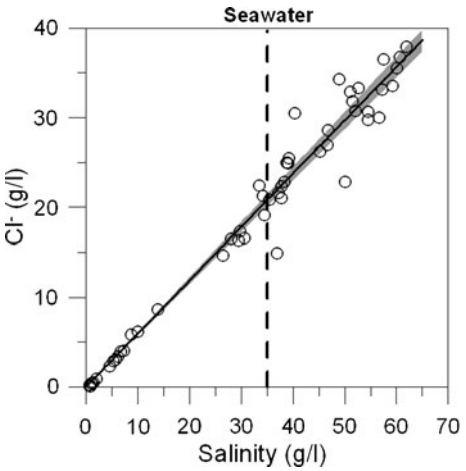

Fig. 5 Plot of MLS salinity versus MLS Cl^- concentration for all groundwater samples (*open circles*). *Solid line* indicates the linear regression line with 95 % confidence intervals (*shaded area*) and *dashed line* shows the limit of seawater salinity

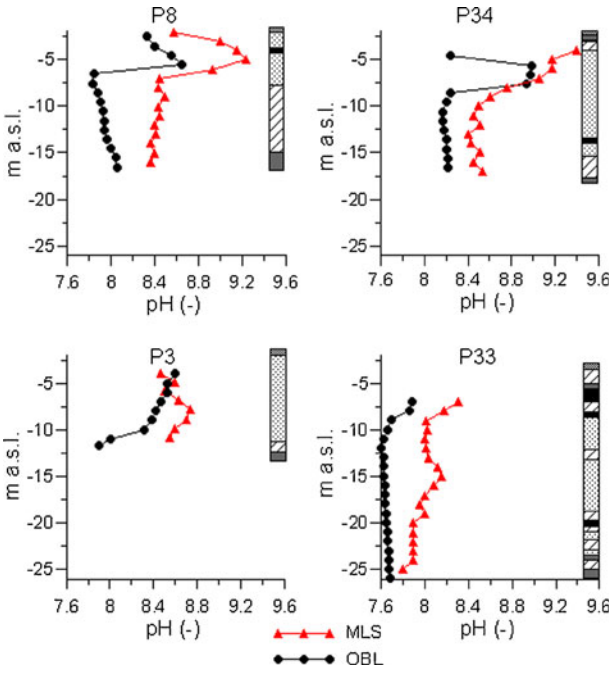

Fig. 6 Plots of pH with MLS versus OBL data for each piezometer along the transect AB; stratigraphy (core logs data) from Fig. 2 is displayed on each plot to assist the interpretation

A sharp pH change is recorded with the OBL technique at the fresh-saltwater interface. On the contrary the MLS profiles display smoother and more regular changes, which can be directly related to recharge from the canals (having a typical pH around 8.4) and to the stratigraphy (*i.e.* in P8 where the sudden increase in pH is imputable to the presence of a peat layer).

From Fig. 6 it is clear that the pH observed with the OBL technique reflects the pH of the stratified water column accumulated in the piezometer, but is not strictly representative of the aquifer pH.

Figure 7 shows the Eh profiles for the selected piezometers. Here the discrepancy between the OBL and MLS technique is even more pronounced, with an absolute residual for all the piezometers of 0.76 mV and an R^2 value of 0.22. The profiles are not only different with respect to the absolute values registered but also that the trends recorded by the two different techniques do not coincide.

In P33 the most negative Eh values coincide with sampling depths at which a strong smell of H_2S was detected during the sampling procedure, so it is worth assuming that sulphate reduction probably takes place at levels where labile organic matter is present.

As with Eh values previously discussed, the agreement between OBL and MLS techniques in O_2 measurement is very low, with an absolute residual for all the piezometers of 0.25 mg/l and an R^2 value of 0.47.

In agreement with the measured negative Eh, the O_2 concentration is always very low in all piezometers (Fig. 8).

Generally the O_2 concentration recorded via MLS is always higher at the top of the aquifer compared to the OBL technique. Oxic conditions in the upper part of the aquifer are due to direct recharge from the canals network, usually showing O_2 concentration around 5 mg/l.

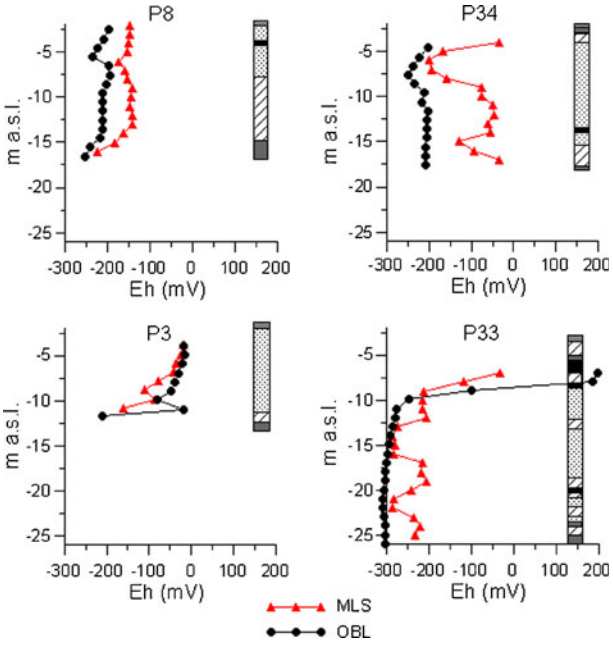

Fig. 7 Plots of Eh with MLS versus OBL data for each piezometer along the transect AB; stratigraphy (core logs data) from Fig. 2 is displayed on each plot to assist the interpretation

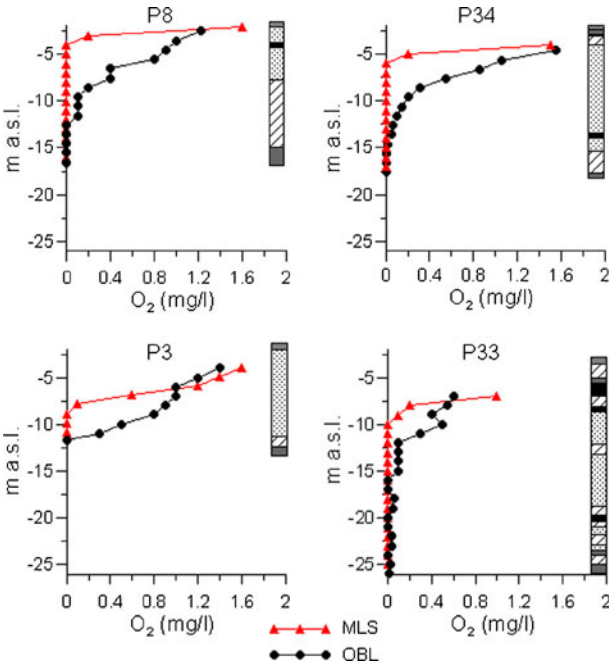

Fig. 8 Plots of O_2 with MLS versus OBL data, for each piezometer along the transect AB; stratigraphy (core logs data) from Fig. 2 is displayed on each plot to assist the interpretation

O_2 concentration recorded via MLS decreases more rapidly with depth with respect to OBL, reaching anoxic condition within 1 to 3 m below the water table. Anoxic values meanwhile are recorded between 4 to 7 m below the water table with the OBL technique.

The reactive sensitive physico-chemical parameter profiles (Figs. 6, 7 and 8) recorded via OBL and MLS techniques give a conflicting overview of the coastal shallow aquifer, as for the salinity values above seawater concentration (Figs. 4 and 5). This means that along this transect, even if the two different acquisition techniques give approximately the same classification and distribution of the water types present in the aquifer, the OBL method cannot be employed to characterize in detail the effects due to interactions between surface and ground waters. The OBL method is also shown to be inappropriate in defining the trend in the redox processes occurring within the aquifer, especially in correspondence with sediments bearing a high content of labile organic matter.

5 Conclusions

This study compares the open-borehole logging (OBL) technique with the more robust but more expensive and time consuming multilevel sampling (MLS) technique. The work shows that, excluding the distribution of saline to hypersaline water types in the bottom part of the aquifer, no significant differences are observed between salinity data recorded by means of the two techniques along the selected transect. It follows that, when the density stratification is from denser groundwater at the bottom to less dense groundwater towards the water table, the OBL method can be successfully used for a preliminary determination of the position of the saltwater wedge and for a general classification and distribution of the water types present in the aquifer.

However, since hydrochemical data (pH, Eh, and O_2) collected with the OBL technique do not agree with data acquired by the MLS technique, a more detailed study on the reactive geochemical processes involving micro and meso-scale structures, like peat layers, can be undertaken only through MLS techniques. Indeed, this study demonstrates that the above even holds when a high level of accuracy in depicting salinity distribution is required in order to infer recharge from surface water bodies. It must be emphasized that in this study the tidal forcing was negligible in most of the investigated piezometers, but tidal effects on groundwater flow should generally be taken into account when monitoring seawater intrusion (especially near to the shoreline) and not immediately ignored.

Acknowledgments Raffaele Pignone, Luciana Bonzi and Lorenzo Calabrese from Geological Survey of Emilia-Romagna Region are acknowledged for their technical and scientific support. Umberto Tessari and Enzo Salemi from Earth Sciences Department of the University of Ferrara are thanked for the grain size analysis. The authors wish to thank Mitchell Dean Harley (University of Ferrara) for his kind contribution in improving the English text.

References

Amorosi A, Centineo MC, Colalongo ML, Pasini G, Sarti G, Vaiani SC (2003) Facies architecture and latest Pleistocene– Holocene depositional history of the Po Delta (Comacchio area), Italy. J Geol 111:39–56

Amorosi A, Centineo MC, Dinelli E, Lucchini F, Tateo F (2002) Geochemical and mineralogical variations as indicators of provenance changes in Late Quaternary deposits of SE Po Plain. Sed Geol 151:273–292

Amorosi A, Colalongo ML, Fiorini F, Fusco F, Pasini G, Vaiani SC, Sarti G (2004) Palaeogeographic and palaeoclimatic evolution of the Po Plain from 150-ky core records. Glob Planet Chang 40:55–78

Antonellini M, Mollema P, Giambastiani BMS, Bishop K, Caruso L, Minchio A, Pellegrini L, Sabia M, Ulazzi E, Gabbianelli G (2008) Salt water intrusion in the coastal aquifer of the southern Po Plain, Italy. Hydrogeol J 16(8):1541–1556

Appelo CAJ, Postma D (2005) Geochemistry, groundwater and pollution, 2nd edn. Balkema, Rotterdam

Balugani E, Antonellini M (2010) Measuring salinity within shallow piezometers: comparison of two field methods. J Water Resour Prot 2:251–258

Balugani E, Antonellini M (2011) Barometric pressure influence on water table fluctuations in coastal aquifers of partially enclosed seas: an example from the Adriatic coast, Italy. J Hydrol 400:176–186

Barlow PM (2003) Ground water in fresh water-salt water environments of the Atlantic Coast. U.S. Geological Survey circular; 1262

Barlow PM, Reichard EG (2010) Saltwater intrusion in coastal regions of North America. Hydrogeol J 18:247–260

Bear J (1972) Dinamics of fluids in porous media. Elsevier, Amsterdam

Bondesan M, Favero V, Vignals MJ (1995) New evidence on the evolution of the Po-delta coastal plain during the Holocene. Quat Int 29(30):105–110

Bonzi L, Calabrese L, Severi P, Vincenzi V (2010) L'acquifero freatico costiero della regione Emilia-Romagna: modello geologico e stato di salinizzazione. Il Geologo dell'Emilia-Romagna—Bollettino Ufficiale d'Informazione dell'Ordine dei Geologi Regione Emilia-Romagna, anno 10/2010 n. 39

Brambati A, Candian C, Bisiacchi G (1973) Fortran IV program for settling tube size analysis using CDC 6200 computer. Istituto di Geologia e Paleontologia, Università di Trieste

Bureau of Reclamation (2001) Water testing for permeability. In: Engineering geology field manual, vol 2, chap 17. US Dept of the Interior, Washington, pp

Candela L, von Igel W, Elorza FJ, Aronica G (2009) Impact assessment of combined climate and management scenarios on groundwater resources and associated wetland (Majorca, Spain). J Hydrol 376(3–4):510–527

Carbognin L, Tosi L (1995) Analysis of actual land subsidence in Venice and its hinterland (Italy). In: Land subsidence. Balkema, Rotterdam, the Netherlands, pp 129–137

Carminati E, Dogliosi C, Scrocca D (2005) Magnitude and causes of natural subsidence of Venice. In: Fletcher C, Spencer T (eds) Flooding and environmental challenges for Venice and its lagoon. Cambridge University Press, Cambridge, pp 21–28

Colombani N, Mastrocicco M, Gargini A, Davis GB, Prommer H (2009) Modelling the fate of styrene in a mixed petroleum hydrocarbon plume. J Cont Hydrol 105(1–2):38–55

Custodio E (2010) Coastal aquifers in Europe: an overview. Hydrogeol J 18:269–280

Danielson RE, Sutherland PL (1986) In: Klute A (ed) Methods of soil analysis, part I. Physical and mineralogical methods, 2nd edn. Agronomy monograph, 9: pp 443–461

Dillon P (2005) Future management of aquifer recharge. Hydrogeol J 13(1):313–316

Gaofeng Z, Yonghong S, Chunlin H, Qi F, Zhiguang L (2010) Hydrogeochemical processes in the groundwater environment of Heihe River Basin, northwest China. Environ Earth Sci 60:139–153

Grassi S, Cortecci G, Squarci P (2007) Groundwater resource degradation in coastal plains: the example of the Cecina area (Tuscany – Central Italy). Appl Geochem 22:2273–2289

Henderson TH, Mayer KU, Parker BL, Al TA (2009) Three-dimensional density-dependent flow and multicomponent reactive transport modeling of chlorinated solvent oxidation by potassium permanganate. J Cont Hydrol 106:195–211

Hill HJ, Shirley OJ, Klein GE (1979) Bound water in shaly sands—its relation to Qv and other formation properties. The log analyst, volume XX(3), Society of professional well log analysts, May–June, 1979, pp 3–19

Jorstad LB, Jankowski J, Acworth RI (2004) Analysis of the distribution of inorganic constituents in a landfill leachate-contaminated aquifer: Astrolabe Park, Sydney, Australia. Environ Geol 46(2):263–272

Kim K-U, Chon C-M, Park K-H, Park Y-S, Woo NC (2008) Multi-depth monitoring of electrical conductivity and temperature of groundwater at a multilayered coastal aquifer: Jeju Island, Korea. Hydrol Processes 22 (18):3724–3733

Kurtzman D, Netzer L, Weisbrod N, Graber E, Ronen D (2011) Steady-state homogeneous approximations of vertical velocity from EC profiles. Ground Water 49(2):275–279

Lenahan MJ, Bristow K (2010) Understanding sub-surface solute distributions and salinization mechanisms in a tropical coastal floodplain groundwater system. J Hydrol 390:131–142

Martinelli L, Zanuttigh B, Corbau C (2010) Assessment of coastal flooding hazard along the Emilia Romagna littoral, IT. Coast Eng 57:1042–1058

National Marine Hydrographic Institute (1994) Istituto Idrografico della Marina, 1994. Tavole di Marea (Mediterraneo – Mar Rosso) e delle correnti di Marea (Venezia – Stretto di Messina), Genova

Nativ R, Weisbrod N (1994) Management of a multilayered coastal aquifer—an Israeli case study. Water Resour Manag 8:297–311

Netzer L, Weisbrod N, Kurtzman D, Nasser A, Graber ER, Ronen D (2011) Observations on vertical variability in groundwater quality: implications for aquifer management. Water Resour Manag 25:1315–1324

Park SC, Yun ST, Chae GT, Yoo IS, Shin KS, Heo CH et al (2005) Regional hydrochemical study on salinization of coastal aquifers, western coastal area of South Korea. J Hydrol 313:182–194

Post V, Abarca E (2010) Preface: saltwater and freshwater interactions in coastal aquifers. Hydrogeol J 18:1–4

Post V, Kooi H, Simmons C (2007) Using hydraulic head measurements in variable-density ground water flow analyses. Ground Water 45(6):664–671

Prommer H, Tuxen N, Bjerg PL (2006) Fringe-controlled natural attenuation of phenoxy acids in a landfill plume: integration of field-scale processes by reactive transport modelling. Environ Sci Technol 40 (15):4732–4738

Schurch M, Buckley D (2002) Integrating geophysical and hydro-chemical borehole-log measurements to characterize the Chalk aquifer, Berkshire, United Kingdom. Hydrogeol J 10(6):610–627

Shalev E, Lazar A, Wollman S, Kington S, Yechieli Y, Gvirtzman H (2009) Biased monitoring of fresh water-salt water mixing zone in coastal aquifers. Ground Water 47(1):49–56

Stefani M, Vincenzi S (2005) The interplay of eustasy, climate and human activity in the late Quaternary depositional evolution and sedimentary architecture of the Po Delta system. Mar Geol 222–223:19–48

Teatini P, Ferronato M, Gambolati G, Gonella M (2006) Groundwater pumping and land subsidence in the Emilia-Romagna coastland, Italy: modeling the past occurrence and the future trend. Water Resour Res 42:1–19

Thierrin J, Davis GB, Barber C (1995) A groundwater tracer test with deuterated compounds for monitoring in situ biodegradation and retardation of aromatic compounds. Ground Water 33(3):469–475

Tiessen H, Moir JO (1993) Total and organic carbon. In: Carte ME (ed) Soil sampling and methods of analysis. Lewis Publishers, Ann Arbor, pp 187–211

Vienken T, Dietrich P (2011) Field evaluation of method for determining hydraulic conductivity from grain size data. J Hydrol 400:58–71

Vukovic M, Soro A (1992) Determination of hydraulic conductivity of porous media from grain-size composition, Water Resour Publ, Highlands Ranch, Colorado, pp 83

Worthington PF (1998) Conjunctive interpretation of core and log data through association of effective and total porosity models. In: Harvey PK, Lovell MA (eds), Core-log integration, geological society. London, Special Publications 136, pp 213–223